Topological analysis of polymeric melts: Chain-length effects and fast-converging estimators for entanglement length

Robert S. Hoy[*]

Materials Research Laboratory, University of California, Santa Barbara, California 93106, USA

Katerina Foteinopoulou

Institute for Optoelectronics and Microsystems (ISOM) and ETSII, Universidad Politécnica de Madrid (UPM),
José Gutiérrez Abascal 2, E-28006 Madrid, Spain

Martin Kröger[†]

Department of Materials, Polymer Physics, ETH Zürich, CH-8093 Zürich, Switzerland

Primitive path analyses of entanglements are performed over a wide range of chain lengths for both bead spring and atomistic polyethylene polymer melts. Estimators for the entanglement length N_e which operate on results for a single chain length N are shown to produce systematic $O(1/N)$ errors. The mathematical roots of these errors are identified as (a) treating chain ends as entanglements and (b) neglecting non-Gaussian corrections to chain and primitive path dimensions. The prefactors for the $O(1/N)$ errors may be large; in general their magnitude depends both on the polymer model and the method used to obtain primitive paths. We propose, derive, and test new estimators which eliminate these systematic errors using information obtainable from the variation in entanglement characteristics with chain length. The new estimators produce accurate results for N_e from marginally entangled systems. Formulas based on direct enumeration of entanglements appear to converge faster and are simpler to apply.

PACS number(s): 83.80.Sg, 83.10.Kn, 83.10.Rs, 81.05.Lg

I. INTRODUCTION

The features of polymer melt rheology are determined primarily by the random-walk-like structure of the constituent chains and the fact that chains cannot cross. The motion of sufficiently long chains is limited by "entanglements" which are topological constraints imposed by the other chains. These become important and dramatically change many melt properties (e.g., diffusivity and viscosity) as the degree of polymerization becomes larger than the "entanglement length" N_e. The value of N_e is both a key quantity measured in mechanical and rheological experiments and a key parameter in tube theories of dense polymeric systems [1].

N_e is usually considered to be a number set by chemistry and thermodynamic conditions (e.g., chain stiffness, concentration, and temperature). It has been empirically related to a "packing" length [2]: $N_e \propto (\rho b^3)^{-2}$ [3], where ρ is the monomer number density and $b^2 = \langle R_{ee}^2/(N-1) \rangle$ is the statistical segment length of chains with end-to-end distance R_{ee} and mean degree of polymerization N. In terms of individual entanglements, N_e is defined as the ratio between N and the mean number of entanglements per chain $\langle Z \rangle$, in the limit of infinite chain length,

$$N_e = \lim_{N \to \infty} \frac{N}{\langle Z \rangle}. \qquad (1)$$

We call a function $\mathcal{N}_e(N)$ an N_e estimate if it has the property

$$\lim_{N \to \infty} \mathcal{N}_e(N) = N_e, \qquad (2)$$

where N_e is a system dependent but N-independent quantity. Comparing Eq. (1) with Eq. (2) does *not* imply choosing $\mathcal{N}_e(N) = N/\langle Z \rangle$. The typical experimental N_e estimate uses the plateau modulus G_N^0 [1],

$$\mathcal{N}_e(N) = \frac{4\rho k_B T}{5 G_N^0}, \qquad (3)$$

where k_B is the Boltzmann constant and T is temperature.

A closely related theoretical construct is the primitive path (PP), defined by Edwards [4] as the shortest path a chain fixed at its ends can follow without crossing any other chains. Rubinstein and Helfand [5] realized that the entanglement network of a system could be obtained by reducing all chains to their PPs simultaneously. Such a reduction process is analytically intractable, but has recently been achieved by computer simulations [6–13], which generate networks of PPs from model polymer melts, glasses, random jammed packings, and solutions. These simulations estimate N_e either from the chain statistics of the PPs [6,8,9] or from direct enumeration of entanglements (contacts between PPs) [7,10–12,14,15], which determines $\langle Z \rangle$.

Chain-statistical and direct enumeration approaches produce different results for N_e for the same atomistic configurations, suggesting that "rheological" and "topological" entanglements are not equivalent [15]. This discrepancy has been attributed to the fact that chemical distances between entanglements are not uniform, but rather are drawn from broad distributions [7,10,14–16], even at equilibrium. Studies of how entanglement properties change with N are there-

[*]Corresponding author. robertscotthoy@gmail.com

[†]http://www.complexfluids.ethz.ch

fore of obvious interest. Moreover, primitive path statistics enter recently developed slip-link-based models [17].

In this paper we seek an "ideal" N_e estimate which approaches N_e at the smallest possible N. There have been several attempts in the literature, summarized below, to derive N_e estimates, but these have all exhibited poor convergence (i.e., by approaching N_e only at large $N \gg N_e$). Molecular dynamics simulation times increase with chain length N approximately as N^5 at large N (relaxation time $\tau \propto N^{3.5}$ times system size $\propto N^{3/2}$), so improved N_e estimates have obvious benefits for computationally efficient determination of N_e. By analyzing a number of coarse-grained and atomistic systems, we find a rather general solution to this problem of setting up a N_e estimator, which allows one to predict N_e from weakly entangled linear polymer melts.

The organization of this paper is as follows. Section II presents the polymer models used here and the topological analysis methods which provide us with the entanglement network (primitive paths). Section III distinguishes between valid and quickly converging (ideal) N_e estimators, and discusses some model- and method-independent issues with existing estimators. Examples are given which highlight systematic errors caused by improper treatment of chain ends and of the non-Gaussian statistics of chains and primitive paths. Section IV derives two (potentially) near-ideal estimators which extract N_e from the variation in entanglement characteristics with N. Section V presents and discusses numerical results for these estimators for two very different model polymers. We verify that they are basically ideal, explain why this is so, and derive simplified forms which further illustrate the connection of N_e to chain structure and entanglement statistics and are also near ideal. Section VI contains conclusions, and two appendixes provide additional technical details.

II. POLYMER MODELS AND METHODS

A. Model polymer systems

We have created thoroughly equilibrated configurations for two very different (but commonly used) model polymer melts; monodisperse "Kremer-Grest" bead-spring chains, and atomistic, polydisperse polyethylene. These two are chosen because they have similar values of N_e but very different chain stiffness constants $C(\infty)$. Polyethylene is much more "tightly entangled" [18] in the sense of having a much lower value of $N_e/C(\infty)$; cf. Tables II and III.

The bead spring model [19] captures the features of polymers which are key to entanglement physics, most importantly chain connectivity/uncrossability. Each chain contains N beads of mass m. All beads interact via the truncated and shifted Lennard-Jones potential $U_{LJ}(r) = 4\epsilon_{LJ}[(\sigma/r)^{12} - (\sigma/r)^6 - (\sigma/r_c)^{12} + (\sigma/r_c)^6]$, where $r_c = 2^{1/6}\sigma$ is the cutoff radius and $U_{LJ}(r) = 0$ for $r > r_c$. Here σ is the bead diameter and ϵ_{LJ} is the binding energy, which are both set to 1; all quantities will thus be dimensionless and given in the conventional Lennard-Jones (LJ) units. Covalent bonds between adjacent monomers on a chain are modeled using the finitely extendable elastic (FENE) potential $U(r) = -\frac{1}{2}kR_0^2 \ln[1 - (r/R_0)^2]$, with the canonical parameter choices $R_0 = 1.5$ and

$k = 30$ [19]. The equilibrium bond length is $l_0 \approx 0.96$. This model is hereafter referred to as the "LJ+FENE" model.

Values of the density and temperature ($\rho = 0.85$ and $T = 1.0$) are those typically used for melt simulations [6,9,19]. All systems contain 280 000 total beads. While all are monodisperse, we employ a wide range of chain lengths, $4 \le N \le 3500$. Those with $N \ge 100$ are equilibrated using the "double-bridging hybrid" (DBH) algorithm [20]. DBH uses molecular dynamics to update monomer positions and Monte Carlo chain-topology-altering moves [21] to overcome the slow diffusive dynamics [1] of entangled chains. All equilibration simulations were performed using the LAMMPS [22] molecular-dynamics code. Reference [19] predicted $N_e \approx 35$ at the above-mentioned state point using various "rheological" measures applied to systems with $N \le 400$, while a similar analysis in [23] predicted $N_e \approx 75$.

In all simulations of the atomistic polyethylene (PE) melt, the united atom representation is adopted. Accordingly, carbon atoms along with their bonded hydrogen atoms are lumped into single spherical interacting sites. There is no distinction between methyl and methylene units in the interaction potentials. All bond lengths are kept constant ($l_0 = 1.54$ Å), while bending and torsion angles are, respectively, governed by harmonic and sum-of-cosine potentials [24,25]. Pair interactions between all intermolecular neighbors, and intramolecular neighbors separated by more than three bonds, are described by the 12–6 Lennard-Jones potential. The parameters of the mathematical formulas for the bonded and nonbonded interactions are given in Refs. [10,21,24,25]. These interaction potentials yield accurate predictions of the volumetric, structural and conformational properties of PE melts over a wide range of chain lengths and temperatures [21,24].

All atomistic PE systems were equilibrated through Monte Carlo (MC) simulations based on advanced chain-connectivity-altering algorithms: the end-bridging [26] and double bridging [21,25] moves along with their intramolecular variants. The simulated systems are characterized by average chain lengths from $N = 24$ up to $N = 1000$, with a small degree of polydispersity. Chain lengths are uniformly distributed over the interval $[(1 - \Delta)N, (1 + \Delta)N]$. Here Δ, the half width of the uniform chain length distribution reduced by N, is 0.5 and 0.4 for $24 \le N \le 224$ and $270 \le N \le 1000$, respectively. More details about the MC scheme, including a full list of moves, attempt probabilities, and acceptance rates, can be found elsewhere [24]. Equilibration at all length scales, which is essential to obtaining meaningful results from entanglement analyses [27], was verified using several metrics [24]. In this study, results are presented for $T = 400$ K and $T = 450$ K, both for $P = 1$ atm.

B. Entanglement network and primitive paths

For the melt configurations the reduction to primitive paths was performed using two methods, PPA and Z, using the procedures described in Refs. [6,7,9,14]. PPA simulations used LAMMPS and Z simulations used the Z1 code [28]. Both PPA and Z1 analyses are performed for the LJ+FENE model, while only Z1 analysis is performed for PE. In both

TABLE I. Chain and primitive path dimensions for PPA and Z1 as well as number of kinks $\langle Z \rangle$ for Z1 for the LJ+FENE polymer melt. All quantities given in reduced LJ units. It is remarkable that values obtained via Z1 and PPA are very comparable, suggesting that chain thickness and slippage effects seem to cancel as discussed in [14].

N	$\langle R_{ee}^2 \rangle$	$\langle L_{pp} \rangle_{PPA}^2$	$\langle L_{pp}^2 \rangle_{PPA}$	$\langle L_{pp} \rangle_{Z1}^2$	$\langle L_{pp}^2 \rangle_{Z1}$	$\langle Z \rangle_{Z1}$
20	29.24	33.18	37.56	28.21	32.16	0.127
28	42.85	51.86	58.66	44.03	50.32	0.287
35	54.69	71.01	79.85	60.52	69.00	0.462
50	80.30	116.2	129.8	100.2	113.9	0.823
70	114.9	193.3	213.4	169.7	190.7	1.337
100	169.1	343.0	373.3	301.8	334.8	1.995
125	215.2	483.7	522.1	431.9	475.4	2.514
140	233.0	593.5	633.2	528.1	576.6	2.876
175	289.5	847.9	900.2	766.5	831.1	3.541
250	421.9	1646	1716	1481	1577	5.089
350	609.4	3143	3245	2764	2907	7.168
500	831.0	6050	6188	5527	5738	10.261
700	1203	1.170×10^4	1.189×10^4	1.057×10^4	1.084×10^4	14.343
875	1521	1.757×10^4	1.779×10^4	1.624×10^4	1.659×10^4	17.793
1750	3003	6.769×10^4	6.806×10^4	6.215×10^4	6.294×10^4	35.204
3500	6157	2.591×10^5	2.599×10^5	2.441×10^5	2.457×10^5	70.444

methods, all chain ends are fixed in space. Intrachain excluded volume interactions are disabled while chain uncrossability is retained. Both classical PPA [6] and geometrical methods (Z1 [7,14] or CReTA [11,15]) provide the configuration of the entanglement network and the contour lengths L_{pp} of each primitive path. In PPA, disabling intrachain excluded volume produces a tensile force [29] in chains which reduces the contour lengths. In Z1, contour lengths are monotonically reduced through geometrical moves in the limit of zero primitive chain thickness. In addition to L_{pp} and the configuration of the entanglement network, Z1 analysis also yields the number of interior "kinks" [7], Z, in the three-dimensional primitive path of each chain. $\langle Z \rangle$ is considered to be proportional to the number of entanglements, regardless of the details of the definition used to define an entanglement.

Runs end when the mean length of the primitive paths, $\langle L_{pp} \rangle$, and/or the mean number of interior kinks per chain, $\langle Z \rangle$, converge. Self-entanglements are neglected, but their number is inconsequential for the systems considered here [9]. The CReTA method works similarly, and the conclusions reached here for Z1 analysis should apply similarly to CReTA results [14,15].

Table I summarizes chain and primitive path dimensions as well as $\langle Z \rangle$ for LJ+FENE chains with $20 \leq N \leq 3500$. Statistically independent initial states were used so that the random error on all quantities is $\lesssim 2.5\%$. It is remarkable that PPA and Z1 data for $\langle L_{pp} \rangle$ and also $\langle L_{pp}^2 \rangle$ are so similar, considering the differences between the contour length reduction methods. Relative to Z1 results, PPA values of $\langle L_{pp} \rangle$ are increased by finite chain thickness effects [11,30] and decreased by chain end slip-off [14]. Both these effects should decrease in strength as N increases, and indeed

$\langle L_{pp}^2 \rangle_{PPA}/\langle L_{pp}^2 \rangle_{Z1}$ decreases from ~ 1.17 to ~ 1.06 over the range $20 \leq N \leq 3500$. A very comparable trend is offered by $\langle L_{pp} \rangle_{PPA}^2 / \langle L_{pp} \rangle_{Z1}^2$.

PPA results for the shortest chains ($N < 20$) are not presented. Standard PPA is unreliable for very short chains because the presence of a high concentration of fixed chain ends combined with the finite bead diameter effectively inhibits relaxation [11,30]. These problems are even worse for topological analysis of lattice polymer systems—see, e.g., Ref. [12]. In the following, where (as will be shown) accurate data from very short chains are important, we focus on Z1 results.

III. TOWARD VALID ESTIMATORS

A basic task of topological analysis is to calculate N_e from the full microscopic configuration of the entanglement network. The simplest approaches employ only the mean-square end-to-end distance of chains $\langle R_{ee}^2 \rangle$ and either the mean length of the primitive paths $\langle L_{pp} \rangle$ or the mean number of kinks $\langle Z \rangle$. Notice that $\langle Z \rangle$ is not an integer, but semipositive, $\langle Z \rangle \geq 0$. In order to estimate N_e from weakly entangled systems one of course needs physical insight; when this is limited, a good N_e estimator can only be guessed.

Some restrictions arise from a purely mathematical viewpoint. A valid estimator $\mathcal{N}_e(N)$ has the following properties:

(i) It obeys Eq. (2) and uses information from polymer configurations whose mean chain length does not exceed N;

(ii) It either yields $\mathcal{N}_e(N) \geq N$ or leaves $\mathcal{N}_e(N)$ undefined for a system of completely unentangled ($\langle Z \rangle = 0$) chains;

(iii) An "ideal" estimator we define to correctly predict N_e for all N exceeding N_e, or for all $\langle Z \rangle$ exceeding unity.

Accordingly, for an ideal estimator, the following weaker conditions hold:

(iv) An ideal estimator diverges for a system of rodlike chains possessing $N_e = \infty$, and

(v) It exhibits $\mathcal{N}_e(N) \leq N$ when each chain has in average more than a single entanglement, $\langle Z \rangle > 1$.

The following two subsections repeat earlier approaches to estimate N_e. Basic considerations of finite chain length effects, errors from improper treatment of non-Gaussian structure, and the general behavior of quantities entering N_e are discussed. These subsections are meant to prepare the reader for the ideal estimators to be presented in Sec. IV. They reflect the chronology of our search for better estimators and help the reader to understand the magnitude of improvements presented in Sec. V. The arguments given here ultimately point the way to construct ideal estimators.

A. Nonideal estimators

Modeling primitive paths as random walks, Everaers *et al.* [6] developed an estimator (which we denote as "classical S-coil") which operates on results for configurations ("coils") of a single (S) chain length,

$$\mathcal{N}_e(N) = (N-1)\frac{\langle R_{ee}^2 \rangle}{\langle L_{pp} \rangle^2}. \tag{4}$$

The classical S-coil estimate (4) is useful because (for long chains) it relates changes in chain structure to rheological trends [6,18]. However, while it fulfills basic requirements (i) and (ii) (both unentangled and rodlike chains have $R_{ee} = L_{pp}$), it lacks properties (iii) and (iv). As the exact relation of $\langle R_{ee}^2 \rangle / \langle L_{pp} \rangle^2$ and $\langle Z \rangle$ is unknown, it is *a priori* unclear whether it has property (v).

The corresponding estimator operating on the number of kinks, $\langle Z \rangle$, and originally employed in [7], denoted here as "classical S-kink," is

$$\mathcal{N}_e(N) = \frac{N(N-1)}{\langle Z \rangle (N-1) + N}, \tag{5}$$

which fulfills the basic requirements (i) and (ii), and also (v), but lacks (iii) according to Ref. [10] and (iv) by definition. The presence of both $N-1$ and N in Eqs. (4) and (5), and subsequent estimators reflects the fact that it is the existence of a bond rather than a bead which is responsible for the presence or absence of an entanglement between two chain contours.

The performance of the two classical estimators (4) and (5) for the two polymer models considered here is illustrated in Fig. 1. Values of $\mathcal{N}_e(N)$ converge very slowly with increasing N. As expected from their form, but contrary to both rheological intuition and condition (ii), values of $\mathcal{N}_e(N)$ drop strongly with decreasing N. For marginally entangled chains (where N is just large enough so that $\langle Z \rangle$ is small but nonzero), both classical estimators yield $\mathcal{N}_e(N) \leq N-1$. For example, for $N=20$, they both predict $\mathcal{N}_e(N)=17$, which is close to the (improper) upper bound $N-1=19$. This prediction obviously has no connection to the actual topology of the system.
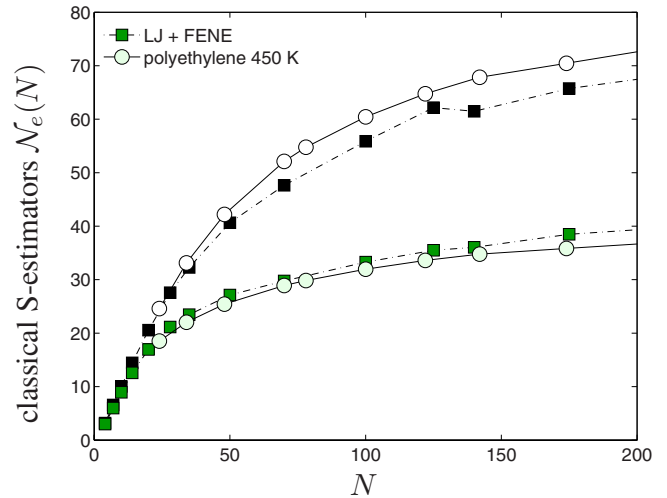

FIG. 1. (Color online) Performance of classical N_e estimators $\mathcal{N}_e(N)$ based on coils (4) (upper two curves) and kinks (5). Data are shown for the two model polymer melts studied in this manuscript. The trends with N are in agreement with published results for other systems [7,10,11,14,31–33]. The convergence behavior is poor, as $N_e \equiv \lim_{N \to \infty} \mathcal{N}_e(N)$ obviously cannot be extrapolated studying chains with $N < 100$, while N_e turns out to stay well below 100 for both systems. An "ideal estimator," as defined in Sec. III, would converge when N exceeds N_e or earlier.

Thus Eqs. (4) and (5) always underestimate, but never overestimate N_e. This feature of the two estimators in the limit of unentangled chains is particularly (if retrospectively) disappointing, as it is incompatible with goal (iii). Similar behavior was reported (but not analyzed as in this paper) in Refs. [31–33].

Other previously published N_e estimators [9,11,16,34] also have some, but not all, of properties (i)–(v). One of the most promising was proposed in Ref. [9]. It estimates N_e from the *internal* statistics of primitive paths, for a single N. The squared Euclidean distances $\langle R^2(n) \rangle$ between monomers separated by chemical distance $n \leq N-1$ *after* topological analysis (i.e., the chain statistics of the primitive paths) were fit [9] to those of a freely rotating chain with fixed bond length fixed bending angle. N_e was then identified with the chain stiffness constant $C(\infty)$ of the freely rotating chain [35]. This estimator does not *obviously* fail to meet any of conditions (i)–(v). In Ref. [9] it gave values of $\mathcal{N}_e(N)$, which decreased more slowly than Eq. (4) as N decreased. Unfortunately, its predictions agree with Eq. (4) at moderate $N \gtrsim 100$ and thus it fails condition (iii).

New S estimators based on modifications to Eqs. (4) and (5) may be proposed. During the course of developing ideal estimators (to be introduced in Sec. IV), we developed two modified single chain length estimators which tend to approach N_e from above rather than from below. These are the "modified S-kink" estimator,

$$\mathcal{N}_e(N) = \frac{N}{\langle Z \rangle}, \tag{6}$$

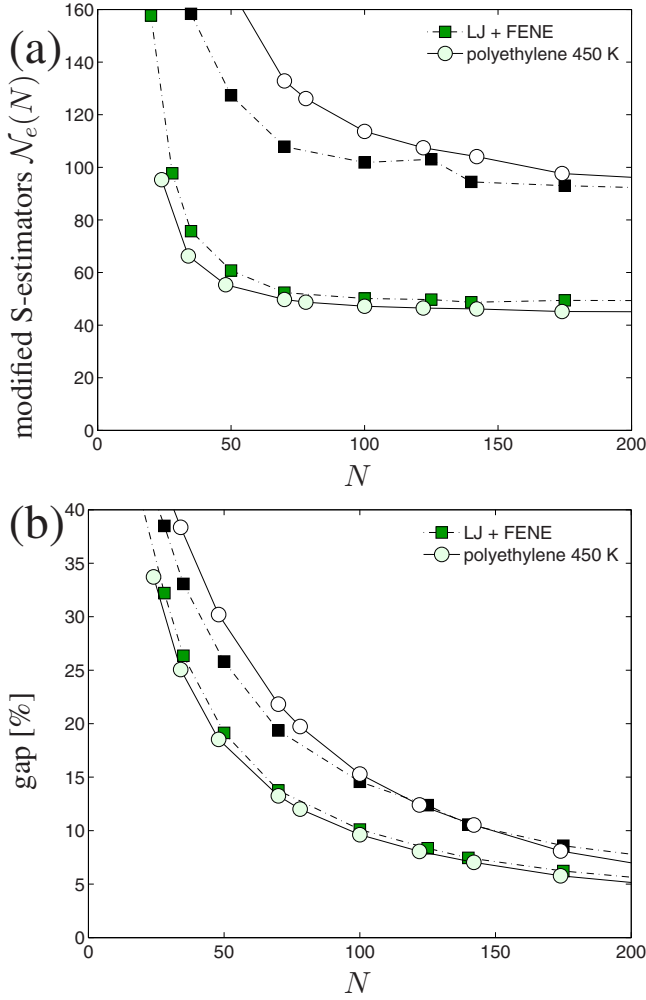and the mathematically similar "modified S-coil" estimator

FIG. 2. (Color online) (a) Performance of modified S-kink estimator (6) (lower two curves) and the modified S-coil (7) (upper two curves). which approach N_e from above. Data are for the same systems analyzed in Fig. 1. The single-configuration estimator for kinks exhibits an improved convergence behavior compared with Eq. (5). Under circumstances discussed in Sec. V, application of both modified and original classical estimators allows one to obtain lower and upper bounds on N_e which tighten with increasing N. (b) Shown are the relative differences ("gap [%]") between $\mathcal{N}_e(N)$ values shown in Fig. 1 and the ones plotted in part (a) of the current graph. Differences are smaller for N_e estimated from kinks (lower two curves).

$$\mathcal{N}_e(N) = (N-1)\left(\frac{\langle L_{pp}^2 \rangle}{\langle R_{ee}^2 \rangle} - 1\right)^{-1}. \qquad (7)$$

A motivation for the use of $\langle L_{pp}^2 \rangle$ rather than $\langle L_{pp} \rangle^2$ in Eq. (7) appears in Appendix A. Figure 2 shows results for Eqs. (6) and (7) for the same systems analyzed in Fig. 1. Both modified single-chain estimators give $\mathcal{N}_e(N) = \infty$ for unentangled chains, thus fulfilling criterion (iv) in addition to (i) and (ii), but they still fail to fulfill goal (iii) since they tend to overestimate N_e for weakly entangled chains.

B. Errors from improper treatment of non-Gaussian structure and chain ends

Critically, none of the above-mentioned estimators seem to be able to predict $\mathcal{N}_e(N) = N_e$ for weakly entangled systems with a slightly positive $\langle Z \rangle \lesssim 1$. All above-cited previous works as well as Eq. (7) have only produced convergence for $N \gg N_e$, and we are not aware of any studies where convergence has been achieved at $N \approx N_e$, i.e., we are not aware of the former existence of any ideal N_e estimator. However, the failure of so many previous attempts both makes it worth examining the common reasons why they have failed, and in fact points the way to creating ideal N_e estimators.

To leading order in $\epsilon \equiv (N-1)^{-1}$ (i.e., the inverse number of bonds), data for a wide variety of model polymers (see, e.g., Refs. [20,24,31]), as well as the data obtained in this study [see Fig. 3(a)] are consistent with

$$\langle R_{ee}^2 \rangle(\epsilon) = D/\epsilon - Y, \qquad (8)$$

where the relative magnitudes of the constant coefficients Y and D depend on factors such as chain stiffness, molecular details, and thermodynamic conditions.

Also, orientations of successive PP segments are correlated [11], so $\langle L_{pp} \rangle^2$ should not be simply quadratic in chain length. The expected leading-order behavior of $\langle L_{pp} \rangle^2$ is

$$\langle L_{pp} \rangle^2(\epsilon) = A/\epsilon^2 + B/\epsilon, \qquad (9)$$

where B contains contributions from non-Gaussian statistics and contour length fluctuations [1]. Relationships (8) and (9) are consistent with data reported elsewhere (e.g., Refs. [24,32]) as well with our own data, as shown in Fig. 3.

At this point it is worthwhile to mention that we are going to make use of Eq. (9), which is able to capture our results for $\langle L_{pp}^2 \rangle$ down to chain lengths N small compared with N_e, to devise an ideal estimator in Sec. IV. Relationship (8) however, as we will see, will *not* be required to hold to devise an ideal estimator.

Inserting Eqs. (8) and (9) into the classical and modified S-coil, Eqs. (4) and (7), respectively, give to leading order in ϵ,

$$\mathcal{N}_e(N) \overset{(4)}{=} \frac{D}{A} - \frac{AY+BD}{A^2}\epsilon + O(\epsilon^2), \qquad (10a)$$

$$\mathcal{N}_e(N) \overset{(7)}{=} \frac{D}{A} + \frac{D^2-AY-BD}{A^2}\epsilon + O(\epsilon^2). \qquad (10b)$$

Thus non-Gaussian structure of both chains and primitive paths naturally lead to systematic $O(\epsilon) \simeq O(1/N)$ errors in earlier estimators for N_e [36].

Similarly, $\langle Z \rangle$ necessarily scales as ϵ^{-1} in the $N \to \infty$ limit. In the same spirit as the above analysis, and noting the failure (Fig. 2) of Eqs. (5) and (6) to meet condition (iii), let us hypothesize that finite chain length leads to the leading-order behavior,

$$\langle Z \rangle(\epsilon) = G/\epsilon - H, \qquad (11)$$

where G and H are both positive. This assumption is actually consistent with the data in Table I and previous works [24];

see also Sec. IV. The classical and modified S-kink Eqs. (5) and (6) then become

$$\mathcal{N}_e(N) \stackrel{(11)\text{in}(5)}{=} \frac{1}{G} - \frac{1-G-H}{G^2}\epsilon + O(\epsilon^2), \qquad (12\text{a})$$

$$\mathcal{N}_e(N) \stackrel{(11)\text{in}(6)}{=} \frac{1}{G} + \frac{G+H}{G^2}\epsilon + O(\epsilon^2). \qquad (12\text{b})$$

Again, systematic $O(\epsilon)$ errors are predicted. In this case, however, the source is chains being too short to be in the asymptotic entangled limit defined by Eq. (1).

A key to understanding the failure of previous N_e estimators is that *differences* in the prefactors of the $O(\epsilon)$ errors [Eqs. (10) and (12)] arise from different treatment of chain ends. The classical S-kink Eq. (5) underestimates N_e as long as $G+H<1$, and the modified S-kink Eq. (6) strictly overestimates N_e since both G and H are positive. Similarly, the prefactor $(AY+BD-D^2)/A^2$ [Eq. (10b)] of the systematic $O(\epsilon)$ error in the modified S-coil Eq. (7) contains two contributions of different origins. $(AY+BD)/A^2$ arises from the Gaussian-chain approximation used, while $-D^2/A^2$ arises from the attempt to correct for chain ends effects (i.e., the "−1").

We have determined the coefficients A, B, D, G, H, and Y using all available data from our simulations; their values for both polymer models are shown in Table II. Coincidentally, for LJ+FENE chains, $(AY+BD)/A^2 \simeq 5\times10^3$ and $D^2/A^2 \simeq 7\times10^3$. The systematic $O(\epsilon)$ error for the modified S-coil (7) is actually small for LJ+FENE systems due to the near cancellation of its contributing terms. There is no reason to believe this behavior is general, and tests on additional polymer models would be necessary [36] to better characterize how rapidly the modified S-coil typically converges. However, it is reasonable to expect it typically converges more rapidly than the classical S-coil (4).

Before turning to ideal estimators, we mention that the modified S-kink (6) can be regarded as corrected version of classical S-kink (5), as it eliminates an $O(\epsilon)$ error from the latter, and thus converges faster.

IV. IDEAL ESTIMATORS

Given the prevalence of subtle systematic $O(\epsilon)$ errors in nonideal N_e estimators, it is reasonable to suppose that in developing an ideal estimator, one has the freedom to introduce system-dependent (but N-independent) coefficients,
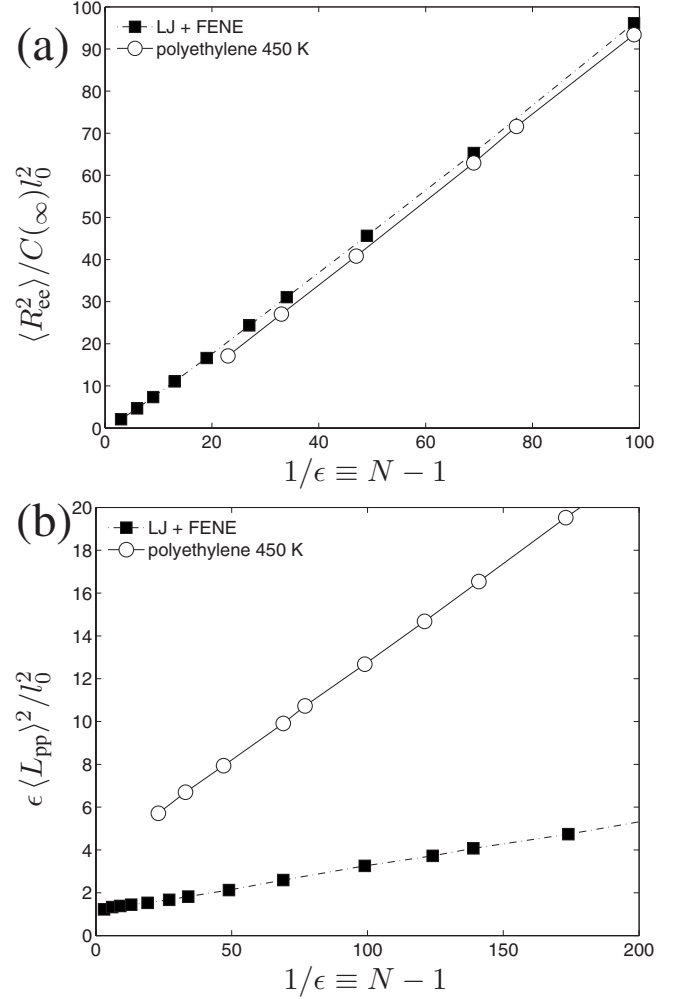

FIG. 3. (a) Testing the applicability of Eq. (8) which predicts linear behavior (slope $\propto D$, offset $\propto Y$) in this representation. We obtain $C(\infty)\approx1.85$ and $C(\infty)\approx8.3$ for the LJ+FENE and PE models, respectively (cf. Table II). (b) Testing the validity of Eq. (9) for both types of melts (slope $\propto A$, offset $\propto B$). The linear relationship is employed to derive estimator (15) in Sec. IV B. (a), (b) Data for larger N are not shown but also agree to all displayed fit lines, to within statistical errors.

e.g., c, c', and Z_0, in equations for a valid $\mathcal{N}_e(N)$ such as $N/\langle Z\rangle+c\epsilon$, $N(1-c'\epsilon)/\langle Z\rangle$, or $N/(\langle Z\rangle+Z_0)$. These formulas are all potentially valid estimators because they fulfill the basic requirement [Eq. (2)]. The coefficients are somewhat related to each other, but have slightly different physical

TABLE II. Data obtained via Z1. The coefficients D, Y, A, and B have been obtained from a least square fit to the available data (covering $N\gg N_e$) for $\langle R_{ee}^2\rangle$ and $\langle L_{pp}\rangle$, according to Eqs. (8) and (9). Similarly, coefficients G and H derive from the measured $\langle Z\rangle$ via Eq. (11).

System	l_0	$C(\infty)$	D	Y	A	B	G	H
			cf. Eq. (8)		cf. Eq. (9)		cf. Eq. (11)	
LJ+FENE	0.964	1.852	1.72	3.55	0.020	1.04	0.020	0.12
Polyethylene 450 K	1.54 Å	8.318	19.7 Å^2	131.4 Å^2	0.22 Å^2	8.58 Å^2	0.023	0.20
Polyethylene 400 K	1.54 Å	8.535	20.2 Å^2	85.3 Å^2	0.24 Å^2	9.37 Å^2	0.025	0.19

meanings. They fulfill conditions (i) and (ii) for arbitrary c and c', but only if $Z_0 \lesssim 1$. Note that finding an ideal N_e estimator neither depends on the interpretation of $\langle Z \rangle$ or requires *a priori* knowledge of the numerical values of the coefficients. However, these numerical values are required to turn the above three expressions into N_e estimates before they can be applied. As these numerical values are certainly sensitive to system features such as chain thickness and stiffness, it is impossible to determine them from a single set of $\langle L_{\rm pp} \rangle$, $\langle R_{\rm ee}^2 \rangle$, and $\langle Z \rangle$ values.

The best possible estimator gives $\mathcal{N}_e(N) = N_e$ for $\langle Z \rangle \ll 1$, but such an estimator would have to rely on incomplete information, some model assumptions, or make use of some "universal" features of entangled systems such as those suggested by Refs. [10,11]. We make use of two such findings (Sec. III): for the polymer models considered here, both $\langle Z \rangle$ and $\langle L_{\rm pp} \rangle^2/(N-1)$ are linear in $(N-1)$ above certain characteristic thresholds. Further supporting data for atomistic polyethylene have been reported recently [24].

For both models considered here, the "characteristic thresholds" are located at $\langle Z \rangle < 1$ and $N < N_e$, allowing us to make use of the "linearities" to construct ideal N_e estimators. We now derive two near-ideal N_e estimators for kinks and coils, respectively. These estimators operate on multiple (M) systems with different chain lengths, rather than on a single configuration, and will be denoted as M-coil and M-kink in order to clearly distinguish between S and M estimators. Careful empirical tests of the new estimators' validity is quite essential, and will be given in Sec. V.

Below, the idea behind the different roles of Eqs. (8), (9), and (11) is that the statistics of the entanglement network can be expected to be decoupled from the fractal dimension of the atomistic chain because entanglements arise from interchain rather than intrachain configurational properties. The estimator we develop in the following section will, in fact, potentially be applicable to non-Gaussian chains, where $\langle R_{\rm ee}^2 \rangle \propto \epsilon^{-\mu}$ (with $1 \leq \mu \leq 2$), as well as less-flexible polymers (like actin [37] or dendronized polymers [38]) for which N_e is [18] of the order of a "persistence length" of the atomistic chain.

A. M-kink estimator

Beyond some *a priori* unknown chain length N_1, we know that $\langle Z \rangle$ (as determined via Z1 or CReTA) varies linearly with N, i.e., $\langle Z \rangle = GN + Z_0$ [with $G > 0$, and $Z_0 \equiv -(G+H) > -1$ in the notation of Eq. (11)]. We recall that an ideal N_e estimator implies, according to condition (iii), that

(vi) $d\mathcal{N}_e(N)/dN = 0$ for $N \geq N_1$, and

(vii) $N_1 < N_e$

are necessary to produce $N_e = \mathcal{N}_e(N_1)$. Uniquely, $N_e = 1/G$ and $\mathcal{N}_e(N) = N_e$ for all $N > N_1$. Using the linear relationship between $\langle Z \rangle$ and N we thus propose (a) $\mathcal{N}_e(N) = N/(\langle Z \rangle - Z_0)$, where $Z_0 = Z_0(N)$ is the coefficient determined from data collected up to chain length N. Note that (a) is identical with the N_e estimator suggested on mathematical grounds at the beginning of this section.

However, $\mathcal{N}_e(N) = 1/G$ can be equivalently obtained from (b) $\mathcal{N}_e(N) = dN/d\langle Z \rangle$. This is an estimator, denoted as "M-kink," of extraordinary simplicity,
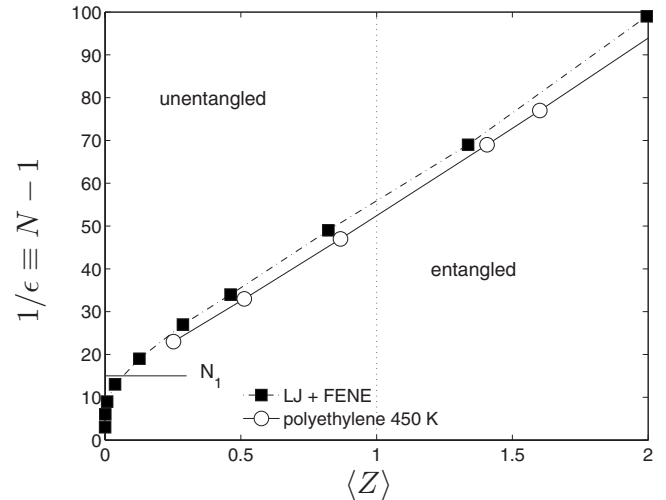

FIG. 4. Z1 results for the two model polymer melts. Testing the applicability of Eq. (11) which predicts linear behavior in this representation (slope G, offset H). Clearly $\langle Z \rangle(N)$ becomes linear at an N for which $\langle Z \rangle < 1$. This implies $N_1 < N_e$ and that Eq. (13) can be an ideal estimator. An interpretation for N_1 is given in Sec. IV A. Data for larger N are not shown here, but the slope $d\langle Z \rangle/dN$ does not change significantly with increasing N.

$$\frac{1}{\mathcal{N}_e(N)} = \frac{d\langle Z \rangle}{dN}. \tag{13}$$

M-kink is strictly an ideal estimator (i.e., it satisfies all five conditions proposed in Sec. III) provided $N_1 < N_e$. It eliminates the unknown coefficient in the linear relationship, and identifies N_e to be responsible for the ultimate *slope* of $\langle Z \rangle(N)$. This is analogous with measurements of diffusion coefficients, where one eliminates ballistic and other contributions by taking a derivative. Application of Eq. (13) requires studying more than a single chain length, which renders our M-kink estimator qualitatively different from the S-kink estimators. Data for $\langle Z \rangle(N)$ for both polymer models, shown in Fig. 4, demonstrate that $\langle Z \rangle$ in fact becomes linear in N for $\langle Z \rangle$ below unity [24,39], thus confirming $N_1 < N_e$. This suggests that N_e can be estimated using data for $\langle Z \rangle$ from chains of lengths even below N_e.

The occurrence of a nonvanishing N_1 is rooted in the fact that a minimum polymeric contour length (of the order of $2\pi\ell$ with polymer thickness ℓ, subsequently corrected by chemical details) is needed for geometrical reasons to form an entanglement (or tight knot) [40]. This length (ℓ) increases with the persistence length of the atomistic contour, and vanishes in the limit of infinitely thin polymers. This implies that determining N_e from the slope we correct for a thickness effect, and N_1 is proportional to the thickness of the atomistic polymer.

B. M-coil estimator

Next, we motivate and derive a near-ideal estimator for use with coil properties $\langle R_{\rm ee}^2 \rangle$ and $\langle L_{\rm pp} \rangle$ (obtained via PPA, CReTA, or Z1). Flory's characteristic ratio $C(N)$ is defined through the identity [41,42]

$$\langle R_{ee}^2 \rangle \equiv (N-1)l_0^2 C(N). \qquad (14)$$

Equation (14) is exact by construction; the N dependence of $C(N)$ characterizes the (non-)Gaussian structure of chains. In general, $C(N) \geq 1$ if $N > 1$. For (mathematically) ideal chains, $C(N)$ is related to the persistence length l_p [35]. This allows the chain stiffness constant $C(\infty) \equiv \lim_{N \to \infty} C(N)$ to be calculated from short chains for any sort of ideal chain, including random walks, freely rotating chains, wormlike chains, etc. Simulations on dense chain packings show [43] that the value of $C(\infty) = 1.48$ is a universal lower limit for excluded volume, flexible chain molecules. For real chains like polyethylene, chains much longer than l_p need to be studied to characterize $C(N)$, cf. Ref. [24]. We assume knowledge of $C(N)$ as function of N from the atomistic configurations.

To proceed, we make use of our finding that $\langle L_{pp} \rangle^2 / (N-1)$ is linear in N above a certain characteristic N_0, before $\langle Z \rangle(N)$ has reached unity, i.e., we assume $N_0 \leq N_e$ to derive an ideal estimator (15). The linear relationship clearly holds for both polymer models considered here [Ref. [24], Table I, Figs. 3(b) and 4], and has already been formulated in Eq. (9). Next we relate $\langle L_{pp} \rangle$ and $\langle Z \rangle$ for large $N \gg N_e$ by a simple argument: the length of the primitive path, L_{pp}, is [18] the number of "entanglement nodes," N/N_e, times the mean *Euclidean* distance ℓ_e between such nodes. This distance (ℓ_e) equals the mean end-to-end distance of the atomistic chain with N_e monomers. We thus expect that up to a factor of order unity (related to fluctuations in ℓ_e [35]), $\lim_{N \to \infty} \langle L_{pp} \rangle^2 = (N/N_e)^2 (N_e - 1) l_0^2 C(N_e)$.

By following the procedure of Sec. IV A, we arrive at an N_e estimator, denoted as "M-coil," using coil properties alone,

$$\left(\frac{C(x)}{x} \right)_{x = \mathcal{N}_e(N)} = \frac{d}{dN} \left(\frac{\langle L_{pp} \rangle^2}{R_{RW}^2} \right), \qquad (15)$$

where $R_{RW}^2 \equiv (N-1)l_0^2$, and $C(x)$ is the characteristic ratio for a chain with $\mathcal{N}_e(N)$ monomers. This estimator fulfills all conditions from our above definition of an ideal estimator. As for M-kink, the derivative in the M-coil Eq. (15) signals that we have to measure $\langle L_{pp} \rangle$ as function of N rather than a single value to estimate N_e. The convergence properties are not as clear *a priori* as they are for the M-kink estimator Eq. (13), as this derivation required an approximation. In practice, one must simulate systems with increasing N until the M-coil converges. There is no apparent way to come up with an N_e estimator from *coil* quantities which converges before N reaches N_e. This is a noticeable difference between the estimators from coils and kinks (M-kink). Technical considerations in the application of Eq. (15) are discussed in Appendix B.

V. NUMERICAL RESULTS AND DISCUSSION

The data in Table I and a similar set for atomistic polyethylene (configurations from Ref. [24]), will now be used to test the M estimators. Figure 5 shows results for the M-kink estimator [Eq. (13)] and M-coil estimator [Eq. (15)] for the same systems analyzed in Figs. 1 and 2. Comparison of these
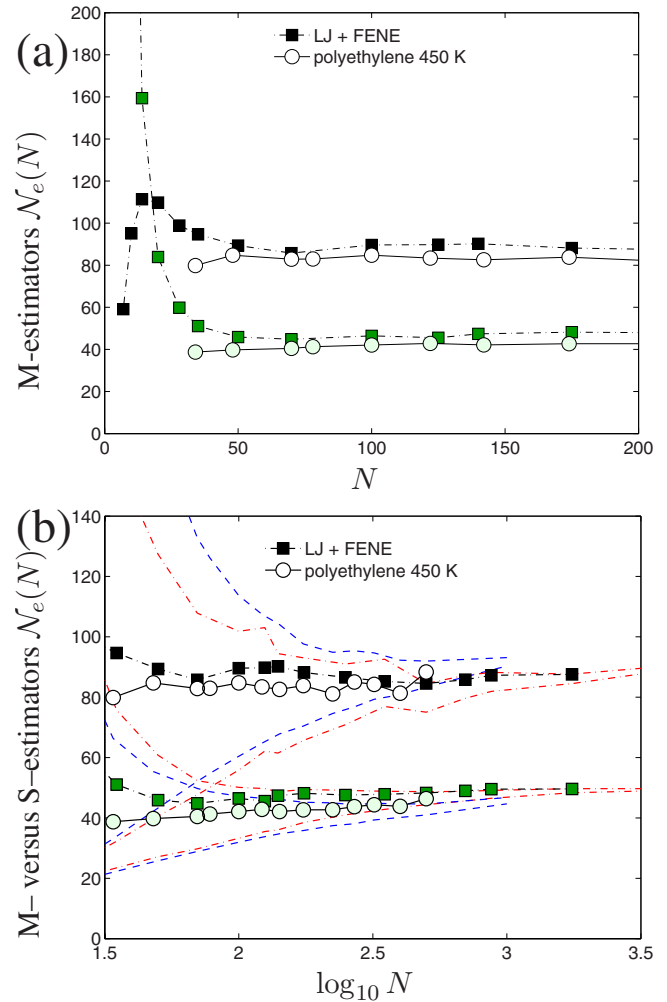

FIG. 5. (Color online) (a) Performance of proposed estimators M-kink (13) (lower two curves with large symbols) and M-coil (15) (upper two curves with large symbols); see also Appendix B. Data are for the same systems analyzed in Figs. 1 and 2. Clearly, $\mathcal{N}_e(N)$ has converged for $N \leqslant 100$, and as shown by comparison to Fig. 4, $\mathcal{N}_e(N)$ approaches N_e before $\langle Z \rangle$ exceeds unity. This allows us to estimate N_e from mostly unentangled systems. (b) Same data as in (a) vs $\log_{10} N$, which allows the full range of N to be presented. For comparison, blue broken and red dashed lines for PE and LJ +FENE, respectively, show reference data for S estimators, already presented in Figs. 1 and 2.

figures shows that the M estimators indeed converge faster than the S estimators [Eqs. (4)–(7)]. Moreover, comparison to Fig. 4 shows that the M estimators converge for marginally entangled systems; values of $\mathcal{N}_e(N)$ approach N_e before $\langle Z \rangle$ far exceeds unity. These show that Eqs. (13) and (15) are essentially "ideal," meeting all of conditions (i)–(v). The kink estimator performs slightly better, presumably because of the approximations made in deriving Eq. (15).

For LJ+FENE systems with $N < 50$, values of $\mathcal{N}_e(N)$ from M-kink (13) increase with decreasing N. As shown in Fig. 5, $\mathcal{N}_e(N)$ appears to be diverging as $N \to 0$. The precise nature of the divergence is unimportant. For example, $N = 20$ chains have $\langle Z \rangle = 0.127$, and the vast majority have zero entanglements, so the prediction $\mathcal{N}_e(20) = 192 \gg 20$ of modified S-kink (6) just signals that we are deep in the unen-

TABLE III. Data obtained via Z1. Selected results for $\mathcal{N}_e(N)$ for all near-ideal M-coil and M-kink estimators defined in this manuscript. For each estimator, two characteristic values are shown: N_e uses all available N (up to $N=3500$ and $N=1000$ for the LJ+FENE and PE models, respectively), and $\mathcal{N}_e(N_e)$ uses only data from short chains with $N \lesssim N_e$ (cf. Table I). Values of $\mathcal{N}_e(N_e)$ are thus obtained at moderate computational cost, and are all in overall agreement with N_e. Approximate M-coil (M-kink) results should coincide with M-coil (M-kink) results, if the relationships (8), (9), and (11), respectively, accurately hold. The simplified M-coil does not take into account the effect of $C(N)$. M-coil (M-kink) is the estimator with the least assumptions involved, if N_e needs to be estimated from coil (kink) information (see also Appendix B). The fact that for all these estimators $\mathcal{N}_e(N_e) \approx N_e$ gives sufficient evidence that these are in fact ideal estimators, in sharp contrast to most S estimators, quantitatively discussed in Table IV. Note that the very similar values of N_e reported for LJ+FENE and PE systems are a pure coincidence arising from their similar values of D/A [Table II; cf. Eq. (18)].

	N_e	$\mathcal{N}_e(N_e)$	N_e	$\mathcal{N}_e(N_e)$	N_e	$\mathcal{N}_e(N_e)$	N_e	$\mathcal{N}_e(N_e)$	N_e	$\mathcal{N}_e(N_e)$
	M-coil		Approximate M-coil		Simplified M-coil		M-kink		Approximate M-kink	
System	Eq. (15)		Eq. (17)		Eq. (18)		Eq. (13)		Eq. (16)	
LJ+FENE	86.1	87.8	85.1	89.6	86.2	90.1	48.9	46.3	48.5	55.7
Polyethylene 450 K	84.0	83.4	84.4	84.5	90.6	90.1	44.2	42.2	43.3	38.8
Polyethylene 400 K	82.3	80.1	80.5	77.8	83.9	84.1	41.5	38.5	40.1	36.3

tangled regime, where N_e cannot yet be estimated.

The fast convergence of the M-kink estimator can be better understood by plugging Eq. (11) into M-kink (13). This produces a special case of the M-kink estimator, which is only asymptotically correct, and can be used when Eq. (11) holds. We refer to it as the "approximate M-kink" estimator,

$$\mathcal{N}_e(N) \approx \frac{1}{G}. \tag{16}$$

Here, G is the coefficient in the linear relationship between $\langle Z \rangle$ and N obtained from data collected up to chain length N, and thus $\mathcal{N}_e(N)$ depends on N. Note that the derivative with respect to N in Eq. (13) removes the $O(\epsilon)$ errors. This is a major difference with respect to all S estimators (the estimator used in [9] can be considered as intermediate between S and M estimators).

In a similar attempt to rationalize the fast convergence of the M-coil estimator, we insert Eqs. (8) and (9) into Eq. (15). This yields, accordingly, the "approximate M-coil" estimator,

$$\mathcal{N}_e(N) \approx 1 + \frac{D + \sqrt{D^2 - 4AY}}{2A}. \tag{17}$$

Like Eq. (16), Eq. (17) has no $O(\epsilon)$ corrections. Again, this arises from the "M" approach of taking derivatives with respect to N. In both cases, the use of the derivatives removes undesirable effects related to proper treatment of chain ends. The approximate M-coil estimator is related only to the (in general, non-Gaussian) structure of chains and primitive paths. Finally, if the assumptions which lead to Eq. (10) hold, and in order to quantify the contributions to Eq. (17), the above analysis combined with tube-theoretic considerations suggests another estimator, which we refer to as "simplified M-coil,"

$$\mathcal{N}_e(N) \approx \frac{D}{A}. \tag{18}$$

The only dependence on N of the approximate and simplified

estimators, Eqs. (16)–(18), stems from the variation of A, D, G, and Y with N; these coefficients, which are obtained by linear interpolation, must generally be assumed be considered to depend on the available range of studied chain lengths. When the variation in the coefficients is large, these three estimators should not be used.

Note that the simplified M-coil does not agree with M-coil if $C(N_e)$ has not reached $C(\infty)$; though it may converge quickly, it cannot be ideal. For the systems under study, N_e is large enough such that $C(N_e)$ is quite close to $C(\infty)$ [44]. The simplified M-coil has a simple connection to polymer structure and the tube model [1]. $D = C(\infty)l_0^2 = l_0 l_K$, where l_K is the Kuhn length [35]. The tube diameter d_T is given by $d_T^2 = l_0 l_K N_e$, and hence $A = (d_T/N_e)^2$.

Table III quantifies the performance of the new M estimators. The two presented values for each estimator $\mathcal{N}_e(N)$ are the final N_e, obtained by analyzing all available chain lengths, together with the value predicted by the estimator at $N = N_e$ (i.e., at the border between unentangled and entangled regimes, using only chains of length up to $\sim N_e$). For an ideal M estimator these two numbers should be the same within statistical errors, here $\sim 2.5\%$, and N_e should coincide with $\lim_{N \to \infty} N/\langle Z \rangle$. All four M estimators considered here, the complete ones [Eqs. (13) and (15)] as well as their approximate versions [Eqs. (16) and (17)] satisfy these criteria. The simplified M-coil (18) is seen to converge quickly as well, but it does converge to an N_e, which is above the one obtained via M-coil, because Y is positive (Y vanishes for an ideal random walk). Table IV shows corresponding results for the S estimators, which all (as discussed above) are generally nonideal. Still, the modified S-kink turns out to perform very well, simply because $G + H \ll 1$ for our model systems, cf. Table II.

For the LJ+FENE model, while the classical S-coil estimator [Eq. (4)] produces values of N_e consistent with published [9] results, i.e., $N_e \simeq 70$ for $N=350$ and 500, values for these estimates based on the near-ideal M estimators (cf. Table III) and also the modified S-coil (7) rise above 80 for the longest chains considered here. The M estimators based on chain and (Z1) primitive path dimensions converge to the

TABLE IV. Data obtained via Z1. For comparison with Table III. Performance of previous S-coil and S-kink estimators. Accurate N_e values have been overtaken from M-coil and M-kink in Table III. Obviously, $\mathcal{N}_e(N_e)$ is far from being close to N_e in all cases, while the deviations are strongest for the N_e estimates based on coils; the two kink measures seem to at least bracket the true N_e (for the deeper reason that Z_0, introduced in Sec. IV, must obey $Z_0 \in [-1, 0]$).

System	N_e	$\mathcal{N}_e(N_e)$	N_e	$\mathcal{N}_e(N_e)$	N_e	$\mathcal{N}_e(N_e)$	N_e	$\mathcal{N}_e(N_e)$
	Classical S-coil		Modified S-coil		Classical S-kink		Modified S-kink	
	Eq. (4)		Eq. (7)		Eq. (5)		Eq. (6)	
LJ+FENE	86.1	40.0	86.1	129.7	48.9	31.7	48.9	51.2
Polyethylene 450 K	84.0	39.7	84.0	192.8	44.2	30.4	44.2	48.3
Polyethylene 400 K	82.3	37.3	82.3	191.8	41.5	28.8	41.5	44.9

value $N_e \simeq 85$ in the mostly unentangled regime, cf. Table III. Thus all data suggest that the "best" estimate of the entanglement length for flexible chains is well above the previously reported value. This is significant, e.g., for quantifying the ratio N_e/N_c, where N_c is the rheological crossover chain length where zero shear viscosity changes its scaling behavior from Rouse to reptation, and has been estimated as $N_c \approx 100$ [3,45].

One could imagine fitting the squared contour length $\langle L_{pp}^2(n) \rangle$ of primitive path subsections [46] to $\langle L_{pp}^2(n) \rangle = An^2 + Cn$ and attempting to calculate $\mathcal{N}_e(N) = D/A$ by also fitting to $\langle R^2(n) \rangle = Dn - Y$, or developing other improved estimators for N_e based on $\langle R_{ee}^2(n) \rangle$ and $\langle L_{pp}^2(n) \rangle$. However, analysis along these lines failed to produce any estimators better than those described above. In particular, no improvement over the method of Ref. [9] was found.

It is important to notice that our Eq. (15) is *not* compatible with some earlier definitions of $\langle Z \rangle$ from coil quantities, because of the prefactor $C(\infty)/C(N_e)$. This prefactor had usually been omitted or not mentioned since random-walk statistics were clearly a convincing starting point. Assuming Gaussian statistics (constant $C(N)$ for all N) hence underestimates values of N_e calculated from coil properties. This issue is also one of the reasons why the N_e estimates between PPA and geometrical approaches differ. Another reason is given in [29]. Ratios between 1.3 and 2.5 between N_e calculated from kinks and coils have been reported [7,10,11,15]. The presented data exhibits ratios between 1.6 and 2. A third reason that they differ is rooted in the fact that $\langle Z \rangle$ is not [7] uniquely defined from a given shortest, piecewise straight path, as it is returned by Z1 or CReTA. This additional discrepancy can only be resolved by matching results for N_e from kinks and coils, and by comparison with experiments.

The classical S-kink (5) strictly underestimates N_e and the modified S-kink (6) strictly overestimates N_e (since both G and H are positive, and $G + H < 1$).

VI. CONCLUSIONS

Very significantly improved, near-ideal, and apparently polymer-model-independent estimators for N_e were derived in this paper, M-coil [Eq. (15), to be used with PPA, Z1, or CReTA] and M-kink [Eq. (13), Z1 and CReTA only]. They

reduce, under further assumptions which seem valid for the model systems studied here, to approximate M-coil [Eq. (17)], simplified M-coil [Eq. (18)], and approximate M-kink [Eq. (16)]. These estimators require simulation of multiple chain lengths, but have eliminated systematic $O(\epsilon)$ errors present in previous methods. This is important for the design of efficient simulation methods in the field of multiscale modeling of polymer melts.

Furthermore, we have proposed variants of the original estimators. The two main problems with existing estimators were identified as: (i) improper treatment of chain ends, and (ii) nontreatment of the non-Gaussian statistics of chains and primitive paths [36]. Improper handling of thermal fluctuations was an additional problem relevant to very short chains. Issues (i) and (ii) lead to separate independent $O(\epsilon)$ errors. Estimators based on direct enumeration of entanglements lack issue (ii), and so are *fundamentally* advantageous for estimation of N_e. The new "M" estimators proposed here formally correct for the errors arising from effects (i) and (ii). The values of the M-coil and M-kink estimators can be taken as "best estimates" for N_e when results are available for multiple chain lengths. The best estimator when only a single chain length is available is the modified S-kink, Eq. (6).

We have shown that $\epsilon \langle L_{pp} \rangle^2$, $\langle Z \rangle$, and also $\langle R_{ee}^2 \rangle$ are all linear in $1/\epsilon$ (thus linear in N) down to the mostly unentangled regime, and have used this information to derive the M estimators and to improve the earlier ones. All coefficients in these linear relationships have been evaluated and listed in Table II. The prefactors for the above-mentioned $O(\epsilon)$ errors can be large, and depend both on the polymer model and method of topological analysis. These errors can produce large changes in estimates of N_e for values of N typically considered in previous studies (e.g., Refs. [6,12,33]). This is significant in light of attempts to compare PPA results for N_e to values obtained by other methods [6,23,33,47] such as direct rheological measurement of the plateau modulus G_N^0, evolution of the time-dependent structure factor $S(\vec{q}, t)$, and estimation of the disentanglement time $\tau_d \propto (N/N_e)^3$ [1]. Some conclusions of those studies may need to be reevaluated in light of the new data.

The proposed M estimators are estimators which exhibit all features required for an ideal estimator (a term which we made precise in Sec. II), and they have been physically mo-

tivated. They converge to N_e for weakly entangled systems ($N \lesssim N_e$). They leave N_e either undefined or infinite for rod-like chains [because $C(N)=N$ for a rod]. They predict $\mathcal{N}_e(N) \gtrsim N$ for a completely unentangled system, which is characterized by $\langle Z \rangle = 0$ and $L_{pp} = R_{ee}$ in accord with the definition of the primitive path which we have adopted in this work (see [29]). The appearance of the coefficient N_1 suggests that there might be a minimum amount of material, N_1, needed to form a single entanglement (as observed for phantom chains [7]). If so, it can be expected to depend on the thickness of the atomistic chain and its stiffness as well as particle density. We expect our findings to be universal in the sense that they should apply to all sorts of real linear polymer chains in the melt state, and we have verified the assumptions underlying the M estimators by direct comparison with both atomistic semiflexible and coarse-grained flexible polymer melts.

References [11,15] pointed out that primitive paths are not random walks, and that there appears to be more than one "topological" entanglement per "rheological" entanglement; thus it is unsurprising that N_e from coils is significantly larger than N_e from kinks (for details see Ref. [18]). The utility of any topological analysis of chains shorter than N_e remains highly questionable because the chains' dynamics are well described by the Rouse model [1,19] and so they cannot be considered "fully entangled" in any meaningful way. However, it seems that the M estimators developed in this work have the ability to extract information from a partial or even marginal degree of entanglement.

The M estimators could be applied in a postprocessing step on existing configurations. For example, it should be of interest to study the effect of flow and deformation on entanglement network characteristics in order to establish equations of motion for relevant coarse-grained variables characterizing the polymer melt. Shear and elongational flows have been studied for both polymer models considered here, but either Z1 was not yet available at the time of these studies [48], or the chains were [49,50] "too short," i.e., had $\langle Z \rangle \ll 1$.

The apparent ability to accurately estimate N_e even for weakly entangled systems may be useful for atomistic models whose computational cost prohibits equilibrating large-N systems, such as polymers containing bulky side groups. The procedure for removal of the $O(\epsilon)$ systematic errors, while clearly described here, requires performing analyses on a limited number of configurations on a range of chain lengths, which is most easily undertaken for systems composed of "short, but not too short" chains. Independent recent work by Tzoumanekas *et al.* [51] follows a similar approach.
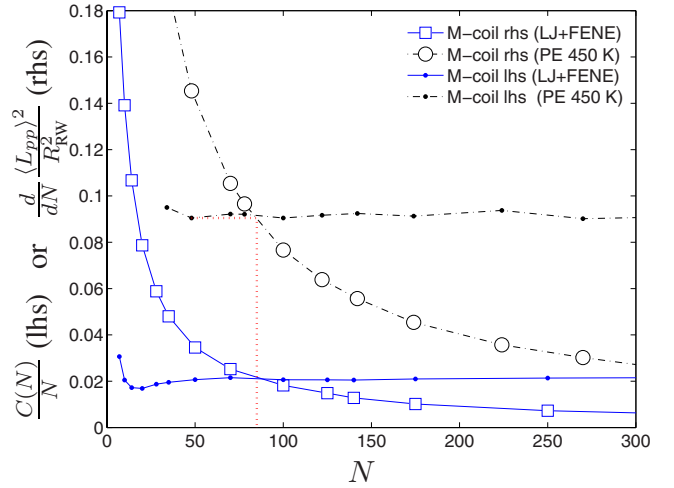
FIG. 6. (Color online) Graphical demonstration of evaluation of $\mathcal{N}_e(N)$ using the M-coil estimator (15). Shown are both the lhs $C(N)/N$, and rhs of Eq. (15) for both types of polymer melts. The dotted (red) path shows how to obtain $\mathcal{N}_e(N) \approx 87$ for a given N; here $N=48$. As described in Appendix B, this value is identical with both N_e and $\mathcal{N}_e(N_e)$, cf. Table III. The ratio $C(N)/N$ (small points) monotonically decreases with increasing N, while the rhs (large symbols) reaches a plateau when N has approached N_e (at the intersection of the curves), which is a distinguishing feature of an ideal estimator.

APPENDIX A: TREATMENT OF THERMAL FLUCTUATIONS

Reference [6] and other studies have typically used $\langle L_{pp} \rangle^2$ rather than $\langle L_{pp}^2 \rangle$ in estimators for N_e, such as the analog for the modified S-coil (7), which reads

$$\mathcal{N}_e(N) = (N-1)\left(\frac{\langle L_{pp}\rangle^2}{\langle R_{ee}^2\rangle} - 1\right)^{-1}. \tag{A1}$$

However, Eq. (A1) gives pathological results for short chains due to thermal fluctuations of L_{pp}. Consider the unentangled limit, where the entanglement density (denoted as ρ_e) vanishes. For an "ideal" topological analysis, $L_{pp} \to R_{ee}$ (from above) for each and every chain as $\rho_e \to 0$. However, chain dimensions fluctuate in thermodynamic equilibrium [1]. To leading order in the fluctuations, $\langle L_{pp}\rangle^2 = \langle L_{pp}^2\rangle - (\Delta L_{pp})^2 \equiv \langle R_{ee}^2\rangle - (\Delta R_{ee})^2$, where Δ is "variance of." So, even for an *ideal* topological analysis procedure, Eq. (A1) would predict a *negative* $\mathcal{N}_e(N) \to -(N-1)\langle R_{ee}^2\rangle/(\Delta R_{ee})^2$ as $\rho_e \to 0$. Negative $\mathcal{N}_e(N)$ are of course useless, but indeed, are predicted using our data in Table I. For $N=20$ (LJ+FENE melt), application of Eq. (A1) yields negative $\mathcal{N}_e(20)$. A term identical to the term in parentheses in Eq. (A1) was found to be

negative for short chains in Ref. [49], but was not used to directly calculate $\mathcal{N}_e(N)$ in their work, as its negative value was considered to signal (and to only occur in) the mostly unentangled regime.

The reason to fix chain ends during PPA or Z1 analysis is the assumption, implicit in Edwards' definition of the primitive path [4], that chains are entangled. In this context it is worthwhile mentioning that there are other definitions of PP's, for example one [52] where the length of the PP goes down to zero for the unentangled chain, and where chain ends are not fixed.

APPENDIX B: TECHNICAL CONSIDERATIONS IN USE OF THE M-COIL ESTIMATOR

While the M-kink estimator [Eq. (13)] is explicitly evaluated from the local derivative $d\langle Z\rangle/dN$ around N, our M-coil expression, Eq. (15), is only an implicit expression for the estimator $\mathcal{N}_e(N)$. Formally, we need the inverse of $C(N)/N$ to calculate $\mathcal{N}_e(N)$. In the following, we describe the procedure in order to prevent any ambiguities upon applying M-coil in practice. Figure 6 shows both the left-hand side (lhs) and right-hand side (rhs) of Eq. (13) versus N for our data. For any given N (say, $N=48$ for the PE data, where the dotted red line starts in Fig. 6), the $\mathcal{N}_e(N)$ estimate is the value at the ordinate for which the abscissa values for lhs and rhs coincide [end of the red curve is at $\mathcal{N}_e(48)\approx87$]. The same procedure is repeated for all N to arrive at Fig. 5 and particular values collected in the M-coil row of Table III. The difference between lhs and rhs can be used to estimate the difference between the largest N available and N_e. If only short chains had been studied, only a part of this plot could have been drawn.

Note that this procedure requires $C(N)/N$ to be monotonically decreasing with N, and access to $C(N)$ at sufficiently large N. While the former is essentially valid for all polymer models, the latter may pose a problem. Without reliable values for $C(N)$ for $N=N_e$, there is no apparent way to come up with an M- coil which converges before N reaches N_e. However, since $C(N)/N$ decreases with increasing N and ultimately reaches $C(\infty)/N$ behavior, in practice (and formally for ideal chains) $C(N)$ can be estimated by extrapolation, and the necessary $C(N)/N$ values could be added for chain lengths exceeding those studied.

This issue disappears by construction when the largest simulated N exceed $\mathcal{N}_e(N)$, so that the conditions for an ideal estimator are met in any case. Still, this is a noticeable and principal difference between the estimators from coils (M-coil) and kinks (M-kink).

---

[1] M. Doi and S. F. Edwards, *The Theory of Polymer Dynamics* (Clarendon, Oxford, NY, 1986).

[2] L. J. Fetters, D. J. Lohse, D. Richter, T. A. Witten, and A. Zirkel, Macromolecules **27**, 4639 (1994); L. J. Fetters, D. J. Lohse, S. T. Milner, and W. W. Graessley, *ibid.* **32**, 6847 (1999).

[3] M. Kröger and S. Hess, Phys. Rev. Lett. **85**, 1128 (2000).

[4] S. F. Edwards, Br. Polym. J. **9**, 140 (1977).

[5] M. Rubinstein and E. Helfand, J. Chem. Phys. **82**, 2477 (1985).

[6] R. Everaers, S. K. Sukumaran, G. S. Grest, C. Svaneborg, A. Sivasubramanian, and K. Kremer, Science **303**, 823 (2004).

[7] M. Kröger, Comput. Phys. Commun. **168**, 209 (2005).

[8] Q. Zhou and R. G. Larson, Macromolecules **38**, 5761 (2005).

[9] S. K. Sukumaran, G. S. Grest, K. Kremer, and R. Everaers, J. Polym. Sci., Part B: Polym. Phys. **43**, 917 (2005).

[10] K. Foteinopoulou *et al.*, Macromolecules **39**, 4207 (2006).

[11] C. Tzoumanekas and D. N. Theodorou, Macromolecules **39**, 4592 (2006).

[12] S. Shanbhag and R. G. Larson, Macromolecules **39**, 2413 (2006).

[13] K. Foteinopoulou, N. Ch. Karayiannis, M. Laso, M. Kröger, and M. L. Mansfield, Phys. Rev. Lett. **101**, 265702 (2008); M. Laso *et al.*, Soft Matter **5**, 1762 (2009).

[14] S. Shanbhag and M. Kröger, Macromolecules **40**, 2897 (2007).

[15] C. Tzoumanekas and D. N. Theodorou, Curr. Opin. Solid State Mater. Sci. **10**, 61 (2006).

[16] M. Kröger, *Models for Polymeric and Anisotropic Liquids* (Springer, Berlin, 2005).

[17] D. Curcó and C. Alemán, Chem. Phys. Lett. **436**, 189 (2007); J. Comput. Chem. **28**, 1929 (2007); J. D. Schieber, D. M. Nair, and T. J. Kitkrailard, J. Rheol. **51**, 1111 (2007); J. D. Schieber, J. Chem. Phys. **118**, 5162 (2003).

[18] N. Uchida, G. S. Grest, and R. Everaers, J. Chem. Phys. **128**, 044902 (2008).

[19] K. Kremer and G. S. Grest, J. Chem. Phys. **92**, 5057 (1990).

[20] R. Auhl, R. Everaers, G. S. Grest, K. Kremer, and S. J. Plimpton, J. Chem. Phys. **119**, 12718 (2003).

[21] N. C. Karayiannis, V. G. Mavrantzas, and D. N. Theodorou, Phys. Rev. Lett. **88**, 105503 (2002).

[22] http://lammps.sandia.gov/

[23] M. Pütz, K. Kremer, and G. S. Grest, Europhys. Lett. **49**, 735 (2000).

[24] K. Foteinopoulou, N. C. Karayiannis, M. Laso, and M. Kröger, J. Phys. Chem. B **113**, 442 (2009).

[25] N. C. Karayiannis, A. E. Giannousaki, V. G. Mavrantzas, and D. N. Theodorou, J. Chem. Phys. **117**, 5465 (2002).

[26] P. V. K. Pant and D. N. Theodorou, Macromolecules **28**, 7224 (1995).

[27] R. S. Hoy and M. O. Robbins, Phys. Rev. E **72**, 061802 (2005).

[28] http://www.complexfluids.ethz.ch/cgi-bin/Z1

[29] In Ref. [6], the primitive path had been defined as the path with minimum elastic energy, rather than the one with shortest length. Larson *et al.* [53] discussed this topic and concluded that methods producing the shortest length paths were preferable. The geometric approaches Z1 [7,14] and CReTA [11] minimize total contour length rather than an elastic energy, and provide us with a shortest parameter-free path.

[30] R. S. Hoy and G. S. Grest, Macromolecules **40**, 8389 (2007).

[31] V. A. Harmandaris and K. Kremer, Macromolecules **42**, 791 (2009).

[32] G. Subramanian and S. Shanbhag, J. Chem. Phys. **129**, 144904 (2008).

[33] S. Leon, N. van der Vegt, L. Delle Site, and K. Kremer, Macromolecules **38**, 8078 (2005).

[34] K. Kamio, K. Moorthi, and D. N. Theodorou, Macromolecules **40**, 710 (2007).

[35] For the case of wormlike (non-Gaussian) chains, $C(N)$ is analytically related to the persistence length l_p of short chains; $C(N+1)=C(\infty)-2\alpha(1-\alpha^N)(1-\alpha)^{-2}/N$, where $\alpha=\exp(-l_0/l_p)$, and $C(\infty)=\lim_{N\to\infty} C(N)=(\alpha+1)/(\alpha-1)$. Note that $\lim_{\alpha\to1} C(N)=N$ and $\lim_{\alpha\to0} C(N)=1$. In the limit $l_p\gg l_0$, the mean-square end-to-end distance of a wormlike chain consequently reads $\langle R_{\rm ee}^2\rangle=2l_pL(1-[l_p/L][1-\exp(-L/l_p)])$ with contour length $L\equiv(N-1)l_0$. In the further limit $L\gg l_p$, $\langle R_{\rm ee}^2\rangle/(N-1)=2l_pl_0=C(\infty)l_0^2\equiv l_Kl_0$, where l_K denotes Kuhn length. These limits are not employed in this work, as we are seeking for corrections in the regime where these limits have not necessarily been reached. For freely rotating chains with a fixed bending angle θ the same result is obtained upon identifying $\alpha=\langle\cos\theta\rangle$. The above expressions for $C(N)$ are directly obtained from a bond–vector correlation function which exponentially decreases with distance between bonds. However, simulations have shown [20] that flexible bead spring chains in melts do not follow this form at small and moderate N. The ratio $C(N)$ must sublinearly and monotonically increase with N in order to uniquely determine N_e from Eq. (15), which limits its use to systems which do not change their statistics on a length scale larger than entanglement length. For the wormlike chain as well as equilibrated bead spring chains [20], $C(N)/N$ decreases monotonically with N.

[36] A. E. Likhtman (private communication). See also Refs. [7,11,20].

[37] J. Kas *et al.*, Biophys. J. **70**, 609 (1996); R. Granek, J. Phys. II **7**, 1761 (1997); S. Ramanathan and D. C. Morse, Phys. Rev. E **76**, 010501(R) (2007).

[38] A. D. Schlüter, Top. Curr. Chem. **245**, 151 (2005); D. K. Christopoulos, A. F. Terzis, A. G. Vanakaras, and D. J. Photinos, J. Chem. Phys. **125**, 204907 (2006); Y. Ding, H. C. Öttinger, A. D. Schlüter, and M. Kröger, *ibid.* **127**, 094904

(2007); M. Kröger, O. Peleg, Y. Ding, and Y. Rabin, Soft Matter **4**, 18 (2008).

[39] Reference [24] reported $N_e>40$ and that $\langle Z\rangle$ became linear at $N>24$.

[40] G. Buck and E. J. Rawdon, Phys. Rev. E **70**, 011803 (2004).

[41] P. J. Flory, *Statistical Mechanics of Chain Molecules* (Wiley, New York, 1969).

[42] M. Rubinstein and R. H. Colby, *Polymer Physics* (Oxford University Press, New York, 2003), p. 53.

[43] N. C. Karayiannis and M. Laso, Phys. Rev. Lett. **100**, 050602 (2008); N. C. Karayiannis, K. Foteinopoulou, and M. Laso, J. Chem. Phys. **130**, 164908 (2009).

[44] A counterexample would be LJ+FENE bead spring chains made semiflexible by the addition of a bending potential $U=-k_\theta\cos(\theta)$; when $k_\theta=2\epsilon_{\rm LJ}$, $C(N_e)$ is still well below $C(\infty)$ [20].

[45] M. Kröger, Appl. Rheol. **5**, 66 (1995); T. Aoyagi and M. Doi, Comput. Theor. Polym. Sci. **10**, 317 (2000).

[46] Unfortunately, this approach can not be used with standard PPA because the tension in the primitive chains produces $\langle L_{\rm pp}^2(n)\rangle\simeq b_{\rm pp}^2n^2$ [8,9], and $\langle L_{\rm pp}^2(n)\rangle=An^2+Cn$ cannot be fit. PPA runs using the linearized-FENE potential of Ref. [8] were also performed, but the performance was poor. In contrast, Z1 and similar methods (e.g., [11]) produce a wide range of local fractional contour length reductions.

[47] A. E. Likhtman, S. K. Sukumaran, and J. Ramirez, Macromolecules **40**, 6748 (2007).

[48] J. Gao and J. H. Weiner, J. Chem. Phys. **97**, 8698 (1992); M. Kröger, W. Loose, and S. Hess, J. Rheol. **37**, 1057 (1993); M. Kröger, C. Luap, and R. Muller, Macromolecules **30**, 526 (1997); P. J. Daivis, M. L. Matin, and B. D. Todd, J. Non-Newtonian Fluid Mech. **111**, 1 (2003).

[49] J. M. Kim, D. J. Keffer, M. Kröger, and B. J. Edwards, J. Non-Newtonian Fluid Mech. **152**, 168 (2008).

[50] J. D. Moore, S. T. Cui, H. D. Cochran, and P. T. Cummings, J. Non-Newtonian Fluid Mech. **93**, 83 (2000).

[51] C. Tzoumanekas, F. Lahmar, B. Rousseau, and D. N. Theodorou, Macromolecules (to be published).

[52] M. Kröger, J. Ramirez, and H. C. Öttinger, Polymer **43**, 477 (2002).

[53] R. G. Larson, Q. Zhou, S. Shanbhag, and S. Park, AIChE J. **53**, 542 (2007).